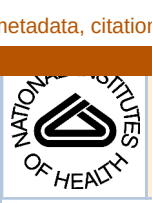

Published in final edited form as:

Development. 2006 July ; 133(13): 2575–2584.

TBX5 is required for embryonic cardiac cell cycle progression

Sarah C. Goetz[1,2], **Daniel D. Brown**[1,2], and **Frank L. Conlon**[1,2,3,*]

1 *Carolina Cardiovascular Biology Center, 5109 Neuroscience Research Building, Chapel Hill, NC 27599-7126, USA.*

2 *Department of Biology, Fordham Hall, UNC-Chapel Hill, Chapel Hill, NC 27599-3280, USA.*

3 *Department of Genetics, Fordham Hall, UNC-Chapel Hill, Chapel Hill, NC 27599-3280, USA.*

Abstract

Despite the critical importance of TBX5 in normal development and disease, relatively little is known about the mechanisms by which TBX5 functions in the embryonic heart. Our present studies demonstrate that TBX5 is necessary to control the length of the embryonic cardiac cell cycle, with depletion of TBX5 leading to cardiac cell cycle arrest in late G_1- or early S-phase. Blocking cell cycle progression by TBX5 depletion leads to a decrease in cardiac cell number, an alteration in the timing of the cardiac differentiation program, defects in cardiac sarcomere formation, and ultimately, to cardiac programmed cell death. In these studies we have also established that terminally differentiated cardiomyocytes retain the capacity to undergo cell division. We further show that TBX5 is sufficient to determine the length of the embryonic cardiac cell cycle and the timing of the cardiac differentiation program. Thus, these studies establish a role for TBX5 in regulating the progression of the cardiac cell cycle.

Keywords

Tbx5; Holt-Oram Syndrome; Cardiogenesis; Cardiac; Heart; Xenopus; Cell cycle; S-phase; Proliferation; T-box

INTRODUCTION

Hyperplastic growth of the vertebrate heart is characterized by two distinct periods of proliferation: one that occurs during early embryogenesis and a second that takes place immediately following birth (MacLellan and Schneider, 2000; Olson and Schneider, 2003; Pasumarthi and Field, 2002). The embryonic phase of cardiac proliferation begins after cardiac cell commitment, and therefore occurs coincident with, or shortly after, gastrulation, a period when the cardiac precursor cells are positioned in two populations on both sides of the organizer or node. Once cells are committed to the cardiac lineage, the two populations of heart precursors migrate to assume their ultimate position along the anterior-ventral midline of the embryo. It is during this narrow window of time that the cardiac precursors undergo rapid cell proliferation to form two epithelial sheets that migrate and fuse, eventually forming the bilaminar heart tube (Fishman and Chien, 1997; Harvey, 2002; Kolker et al., 2000; Mohun et al., 2003; Mohun et al., 2000). During the final stages of migration, the cardiac cells decrease DNA synthesis, gradually withdraw from the cell cycle and initiate terminal differentiation (Pasumarthi and Field, 2002).

*Author for correspondence (e-mail: frank_conlon@med.unc.edu).

During the embryonic stage of cell proliferation, the cardiac cells express the first molecular markers of cardiac development, including *Tbx5*, *Tbx20* and the homolog of the Drosophila *tinman* gene, *Nkx2.5* (Harvey, 2002; Stennard and Harvey, 2005). *Tbx5* is a member of the T-box family of transcription factors, a family of proteins that are required for normal vertebrate patterning and differentiation (Papaioannou and Silver, 1998; Showell et al., 2004; Stennard and Harvey, 2005; Wilson and Conlon, 2002). Clinical studies have provided direct evidence for a role for human *Tbx5* in heart development, with *Tbx5* frequently mutated in patients with the congenital heart disease Holt-Oram syndrome (HOS) (Basson et al., 1997; Li et al., 1997; Mandel et al., 2005). HOS is a highly penetrant autosomal dominant condition that is associated with skeletal and cardiac malformations. The HOS cardiac developmental abnormalities include atrial and ventricular septal defects, as well as conductivity defects and aberrant chamber formation (Basson et al., 1999; Benson et al., 1996; Newbury-Ecob et al., 1996). A role for *Tbx5* in HOS is supported by the observation that mice heterozygous for mutations in *Tbx5* display many of the cardiac abnormalities associated with human patients suffering from HOS (Bruneau et al., 2001). Genetic studies of a *Tbx5* mutation in zebrafish and TBX5 depletion in *Xenopus* are also consistent with a role for TBX5 in heart development (Brown et al., 2005; Garrity et al., 2002; Horb and Thomsen, 1999). The evolutionarily conserved role for *Tbx5* is further emphasized by molecular experiments carried out in tissue culture, zebrafish, *Xenopus*, chicken and mouse, all of which show a role for TBX5 transcriptional activity in regulating the expression of heart-specific genes (Brown et al., 2005; Bruneau et al., 2001; Garrity et al., 2002; Hatcher et al., 2001; Hiroi et al., 2001; Liberatore et al., 2000; Plageman and Yutzey, 2004).

Recently, we have shown that depletion of TBX5 in *Xenopus* leads to profound morphological defects in the heart, including pericardial edema, loss of circulation and a concomitant decrease in cardiac cell number (Brown et al., 2005). In the present study, we demonstrate that the observed decrease in cell number results from defects in embryonic cardiac cell proliferation. We go on to define the expression pattern of an extensive panel of CDK and cyclin proteins in early embryonic cardiac tissue, and show that TBX5 depletion leads to a G_1/S-phase arrest, as demonstrated by a dramatic increase in the expression of proteins associated with the cardiac cell cycle S-phase, including CDC6, cyclin E2, SLBP and PCNA. This suggests that TBX5 is involved in either G_1/S-phase or the early stages of S-phase progression. The G_1/S-phase delay or arrest coincides with a decrease in the embryonic cardiac mitotic index. These events are associated with an alteration in the timing of the cardiac differentiation program, defects in cardiac sarcomere formation and ultimately, cardiac programmed cell death. By contrast, overexpression of *Tbx5*, which we show also leads to heart-specific defects, results in an increase in the cardiac mitotic index and has a converse effect on the timing of the cardiac differentiation program. Collectively, these studies demonstrate that TBX5 is both necessary and sufficient to determine the length of cardiac G_1/S-phase and the timing of the cardiac differentiation program.

MATERIALS AND METHODS

Embryo culture and microinjection

Xenopus embryos and *Xenopus* cardiac actin:GFP transgenic offspring (Latinkic et al., 2002) were prepared and injected as previously described (Wilson and Hemmati-Brivanlou, 1995), and staged according to Nieuwkoop (Nieuwkoop, 1967). For TBX5-depletion studies, embryos were injected with TBX5 and control morpholinos as per Brown and coworkers (Brown et al., 2005). In misexpression studies, capped mRNA for microinjections was generated using the mMessage in-vitro transcription kit (Ambion) according to the manufacturer's instructions. Resulting mRNA was then purified using the RNeasy kit (Qiagen). Embryos were injected with the stated amount of *Tbx5* RNA at the 1-cell stage. Transgenic animals expressing GFP

under the cardiac actin promoter were a generous gift from Dr Tim Mohun (Latinkic et al., 2002).

Immunohistochemistry and whole-mount in-situ hybridization

Embryos were prepared for whole-mount immunohistochemistry according to Kolker and colleagues (Kolker et al., 2000). Briefly, fixed embryos were incubated overnight at 4°C with an antibody against tropomyosin (Developmental Studies Hybridoma Bank), at a dilution of 1:50. Following washes, the embryos were incubated overnight at 4°C with a Cy3-conjugated anti-mouse secondary antibody (Sigma) at a dilution of 1:100. For imaging, embryos were cleared with 2:1 benzyl benzoate: benzyl alcohol and viewed on a Leica MZFLIII fluorescent dissecting microscope. For immunostaining of histological sections, embryos were collected at the indicated stages, fixed for 2 hours in 4% paraformaldehyde, and embedded in OCT cryosectioning medium (Tissue Tek). Cryostat sections (14 μm) were rinsed with wash buffer (PBS with 1% Triton and 1% heat inactivated calf serum), and incubated at 4°C overnight, as indicated, with mouse anti-tropomyosin 1:50, mouse anti-troponin 1:20, mouse anti-fibrillin 1:50 (all from Developmental Studies Hybridoma Bank), mouse anti-MHC (Abcam) rabbit anti-fibronectin 1:50 (Sigma), rabbit anti- Beta-catenin all at 1:1000 (Sigma), rabbit anti-phosphohistone H3 1:50 (Upstate) and rabbit anti-cleaved caspase 3 1:50 (Cell Signaling). The sections were rinsed with wash buffer and the appropriate fluorescent conjugated secondary antibody diluted in wash buffer: anti-mouse-Cy3 1:100 (Sigma), anti-mouse Cy2 1:100 (Jackson), anti-rabbit-Cy3 1:100 (Sigma) and anti-rabbit-FITC 1:150 (Sigma). Samples were incubated for 30 minutes at room temperature with DAPI (Sigma) to stain nuclei, or phalloidin conjugated to Alexa 488 (Molecular Probes, 1:1000) to stain actin filaments. The samples were imaged on a Zeiss LSM410 confocal microscope. Whole-mount in-situ hybridization was performed as previously described (Harland, 1991).

RT-PCR primers

The primers used and cycle number were as follows.

EF1-α F, CCTGAACCACCCAGGCCAGATTGGTG; EF1-α R, AGGTTAGTCAGAGAAGCTCTCCACG (Agius et al., 2000); 25 cycles.

MHC F, GCCAACGCGAACCTCTCCAAGTTCCG; MHC R, GGTCACATTTTATTTCATGCTGGTTAACAGG (Lab designed); 30 cycles.

Muscle actin F, GCTTGTCCCGATCTGAAC; R, TTGCTTGGAGGAGTGTGT (Lab designed); 30 cycles.

MyoD F, AGGTCCAACTGCTCCGACGGCATGAA; R, AGGAGAGAATCCAGTTGATGGAAACA (Hopwood et al., 1989); 25 cycles.

Nkx2.5 F, GAGCTACAGTTGGGTGTGTGTGGT; *Nkx2.5* R, GTGAAGCGACTAGGTATGTGTTCA (DeRobertis, unpublished); 25 cycles.

Tropomyosin F, TGGAGATGGCGGAGAAGAAG; tropomyosin R, GCAGCAAGTGGCAGTCACGA (Charbonnier et al., 2002); 30 cycles.

Troponin I F, GCTGACAGAATGCAGAAG; troponin I R, GAGATTGGCCCGTAGATC (DeRobertis, unpublished); 30 cycles.

All primers were designed to span introns to enable PCR products amplified from cDNA to be distinguished from those amplified by remnant genomic DNA.

RT-PCR reactions

RNA was isolated from five embryos per stage per condition using the RNeasy kit (Qiagen) according to the manufacturer's instructions. The resulting RNA was quantitiated using a UV spectrophotometer (Shimadzu UV-1601), and 100 ng of RNA for each reaction was used to synthesize cDNA with Superscript II reverse transcriptase (Invitrogen). Total reaction volume for cDNA synthesis was 20 μl. Resulting cDNA (2 μl) was then used as template in PCR reactions with Taq polymerase. The number of cycles amplified for each primer (shown above) was determined by running a test PCR reaction and removing an aliquot of each sample after 20, 25, 30 and 35 rounds of amplification to determine the point at which reactions for each primer pair reached saturation. The cycle number used in subsequent experiments for each primer was five amplification cycles prior to the saturation point. For each primer pair, 55°C was used as the annealing temperature.

Western blots

Heart tissue from a minimum of 300 embryos per condition was dissected at stage 33 and snap frozen. Tissue was homogenized, subjected to SDS-PAGE, and transferred according to established protocols. Blots were probed overnight at 4°C with antibodies against Cdc6, Cdt1 [gift from M. Coué, both 1:500 (Whitmire et al., 2002)], cyclin E2 (Abcam, 1:500), PCNA (Zymed, 1:1000), MCM 4 (Abcam, 1:2000), MCM 5 (Abcam 1:400), MCM7 (LabVision, 1:200), Cdk1 (Zymed, 1:1000), Cdk2 (Upstate, 1:1000), cyclin A1, cyclin A2 (Abcam, both 1:1000), SLBP [gift from W. Marzluff, 1:1000 (Wang et al., 1999)], and cyclin B2 [gift from T. Hunt, 1:500 (Hochegger et al., 2001)]. Blots were rinsed and probed with the appropriate HRP-conjugated secondary antibody (Jackson, 1:10,000), and detected with ECL. As a loading control, blots were reprobed with antibodies against Total MEK (Cell Signaling, 1:2000), alpha tubulin (Abcam, 1:1000) and/or SHP2 (BD Biosciences, 1:2500).

Transmission electron microscopy

Stage 37 embryos were fixed in 2% paraformaldehyde/2.5% gluteraldehyde overnight. Embryos were post-fixed in ferrocyanide-reduced osmium and embedded in Spurr's epoxy resin. Transverse ultra-thin (70 nm) sections were mounted on copper grids, and post-stained with 4% aqueous uranyl acetate followed by Reynolds' lead citrate. Sections were imaged with a LEO EM-910 transmission electron microscope.

RESULTS

TBX5 depletion leads to a decrease in cardiac proliferation

To understand the role of TBX5 in heart development, we depleted TBX5 from *Xenopus* embryos using a morpholino-based approach. Results from these studies show that removal of TBX5 leads to morphologically abnormal hearts and a decrease in cardiac cell number that is not associated with a block in cardiac specification, commitment, migration or differentiation (Brown et al., 2005) (Fig. 1A,B). To characterize the phenotype of TBX5-depleted embryos in more detail, and to determine the precise developmental stage at which TBX5 is required during cardiogenesis, we carried out histological analyses and cell-counting studies in TBX5 morpholino-injected (T5MO) and control morpholino-injected (CMO) embryos by double-staining for the cardiac and skeletal muscle marker tropomyosin and with DAPI, to mark cell nuclei (Fig. 1C–F). All cells throughout the heart for each stage were counted, and quantitative results are reported in Fig. 1S. There was no significant difference between control and TBX5-depleted embryos at stage 33 (Fig. 1C,E,S). However, at stage 37 T5MO embryos showed a significant decrease in cardiac cell number compared with their sibling controls (Fig. 1D,F,S). The defect in cell number preceded the expression of proposed TBX5 target genes including atrial naturitic factor (ANF/Nppa) and connexin 40 (Bruneau et al., 2001; Hiroi et al., 2001;

Small and Krieg, 2000). Therefore, the reduction in cardiac cell number appears to be one of the primary cardiac defects in TBX5-depleted embryos.

To determine if the decrease in cardiac cell number is due to cell proliferation or programmed cell death, we analyzed the mitotic index (Fig. 1G–L,T) and apoptosis (Fig. 1M–R,U) at defined time points during heart development: stage 29, which corresponds to the stage when the heart field rounds up to begin forming the bilaminar heart tube; stage 33, at which time cardiac looping is initiated; and stage 37, corresponding to early chamber formation. For these studies CMO and T5MO embryos at each stage were serial-sectioned through the cardiac regions and triple immunostained with anti-tropomyosin (Tmy) to mark cardiomyocytes, DAPI to mark cell nuclei and either anti-phosphohistone H3 (pH3) to mark cells in M-phase (Fig. 1G–L), or anti-cleaved caspase 3 to mark cells undergoing apoptosis (Fig. 1M–R). In each study all cardiomyocytes and endocardial cells encompassed by the cardiomyocytes for each heart at each stage were scored for pH3 or cleaved caspase 3.

CMO embryos showed that the total cardiomyocyte cell numbers underwent a doubling every four stages, or 9 hours, at room temperature between stages 33 and 37 (Fig. 1G–I,M–O). As the majority of the cardiomyocytes appeared to be undergoing mitosis (based on serial sections of multiple embryos at these stages), the embryonic cardiac cell cycle in *Xenopus* was approximately 9 hours in length with M-phase lasting approximately 20 minutes, with the mitotic index gradually decreasing with age (Fig. 1T). We note there was little to no cardiomyocyte programmed cell death during these stages (Fig. 1U).

Results from these studies clearly show a decrease in the mitotic index of T5MO-derived embryos relative to CMO embryos at stage 33 (Fig. 1T); however, no significant programmed cell death was observed until later stages (stage 37; Fig. 1U). As we observed a dramatic decrease in the mitotic index at a time prior to the decrease in cardiac cell number or increases in cardiac programmed cell death (Fig. 1S–U), the primary cause of the reduction in cell number in T5MO cardiac tissue appears to be a decrease in cardiac cell proliferation. Taken together, the data suggest that the decrease in proliferation resulting from depletion of TBX5 is due to either a lengthening of the embryonic cardiac cell cycle or, alternatively, a premature exit of cardiomyocytes from the cell cycle.

TBX5 depletion leads to a cardiac cell cycle delay or arrest in G_1/S-phase

Inference from other systems implies that the integration of growth factor signal cascades with G_1/S cell cycle passage is regulated by the cyclin/CDK complexes CDK2/cyclin E, CDK2/cyclin A and CDK1/cylin D, many of which are expressed in *Xenopus* in a stage-and tissue-specific fashion (Vernon and Philpott, 2003). Although much is known about the cardiac cell cycle during neonatal periods, little is known about the expression of CDKs and cyclins during the early stages of embryonic heart development. To address this issue, we isolated hearts from the first stage at which we could anatomically isolate pure cardiac tissue (stage 33). The resultant tissues were analyzed relative to corresponding whole embryo lysates with an extensive panel of antibodies specific for individual cyclins and CDKs (Fig. 2A). Results from this analysis show that *Xenopus* cardiac tissue at stage 33 expressed cyclin E2, CDC6, PCNA, SLBP, CDK2, cyclin A2 and CDK1, as well as proteins that are expressed uniformly throughout the cell cycle, such as MCM4 and MCM7. Although we could detect high levels of CDT1, cyclin A1, cyclin B2 and MCM5 in stage 33 embryos, we were able to detect little to no expression of these proteins in the heart (Fig. 2A). However, due to the relative amount of cardiac tissue to that of whole embryos, we cannot formally rule out the possibility that these proteins were present at relatively lower amounts. We note that we were unable to identify any antibody that marked D cyclins in *Xenopus*. However, previous studies have suggested that neither of the *Xenopus* D cyclins, cyclin D1 or D2, are expressed in the heart at these stages (Vernon and Philpott, 2003).

We next analyzed cell cycle proteins in heart tissue derived from T5MO and CMO embryos (Fig. 2B). These studies show that depletion of TBX5 led to a dramatic upregulation of the S-phase proteins cyclin E2, CDC6 and CDK2, while proteins associated with other cell cycle phases, cyclin A2 and CDK1, or proteins expressed throughout the cell cycle, such as MCM4 and MCM7, showed no significant differences between T5MO- and CMO-derived heart tissues (Fig. 2B). Together with the mitotic index data, our results strongly suggest that depletion of TBX5 led to a prolonged/arrested G_1- or S-phase and a concomitant decrease in the proportion of cardiac cells in M-phase.

To confirm these findings, we also analyzed CMO- and T5MO-derived hearts for the non-CDK/cyclin S-phase proteins stem loop binding protein (SLBP) and proliferating cell nuclear antigen (PCNA) (Fig. 2C). Western blots of CMO- and T5MO-derived heart tissue show that relative to the loading controls SHP2 and total MEK, depleting TBX5 led to an increase in both SLBP and PCNA levels. Collectively, these results strongly suggest that TBX5 depletion leads to a delay or block in the G_1- or S-phase of the cardiac cell cycle.

Terminally differentiated cardiomyocytes continue to undergo cell division

Our results suggest that TBX5 is required for embryonic cardiac cell cycle progression (Fig. 2) but is not required for cardiac differentiation (e.g. Fig. 1A,B). Thus, terminally differentiated cardiomyocytes could be undergoing cell division or, alternatively, a subpopulation of *Xenopus* cardiomyocytes may undergo cell cycle arrest and terminal differentiation while a second subpopulation of cardiomyocytes continue to divide and remain in an undifferentiated state. The former is consistent with studies in chick and mouse that imply that heart tissue is capable of initiating and maintaining terminal differentiation during a period in which the cells are still dividing, i.e. not during G_1 or G_0 arrest (Anversa and Kajstura, 1998;Burton et al., 1999;Kajstura et al., 2004;McKinsey et al., 2002;Mikawa et al., 1992a;Mikawa et al., 1992b;Rybkin et al., 2003;Soonpaa and Field, 1998). To directly test the relationship between the cardiac cell cycle and terminal differentiation in *Xenopus* embryonic cardiac tissue, we triple-labeled cardiomyocytes at stage 37 with anti-pH3, DAPI and a panel of antibodies that detect terminally differentiated cardiomyocytes, including anti-tropomyosin (Tmy), anti-myosin heavy chain and phalloidin, to mark cardiac actin (Fig. 3). Results from these studies clearly show that in CMO hearts we are able to detect cardiomyocytes that are undergoing mitosis yet also co-express all three markers of terminal differentiation (Fig. 3A–D). In addition, we note that cardiomyocytes expressing tropomyosin, cardiac actin and cardiac myosin heavy chain (MHC) showed the hallmarks of terminal cardiomyocyte differentiation, including the assembly of cells into muscle fibers containing A- and Z-bands. Consistent with findings that fewer cardiac cells in T5MO embryos undergo mitosis (Fig. 1), we were able to detect very few anti-phosphorylated histone H3-positive cells in T5MO-derived hearts. However, of the few cells that expressed pH3, these cells, like controls, also co-expressed markers of cardiomyocyte terminal differentiation, including tropomyosin, actin and MHC (Fig. 3E–H). Taken together, these data indicate that terminally differentiated cells in both control and TBX5-depleted embryos retain the capacity to undergo cell division and suggest that *Xenopus* cardiac cells during these stages do not arrest in G_1 or G_0. These data further suggest that TBX5, although required for cardiac cell cycle progression, is not required to initiate or maintain cardiac differentiation.

TBX5 is required for the proper timing of the cardiac program

As TBX5 depletion does not block cardiac differentiation, we next addressed whether TBX5 depletion could affect the stage at which cardiac markers are initially expressed. To this end, we collected equivalently staged T5MO and CMO embryos at all early stages at which *Tbx5* has been reported to be expressed: stages 10 through 38 (early gastrula through late tadpole). In the first series of studies, we carried out RT-PCR with a panel of primers specific for markers

of cardiac differentiation (cardiac MHC, cardiac troponin and tropomyosin) or skeletal muscle differentiation (MyoD, skeletal muscle actin) (Fig. 4A). Results showed significant differences in the timing of cardiac gene expression in T5MO embryos relative to their stage-matched CMO siblings; T5MO embryos turned on troponin and cardiac MHC at earlier stages than controls (stage 28 in T5MO versus stage 32 in CMO) but initiated expression of Tmy at later stages (stage 24 in T5MO versus 22 in CMO). As we did not observe any changes in the timing at which skeletal muscle markers are expressed, the alteration in timing of differentiation appears to be specific to cardiac tissue.

To confirm these findings, we carried out whole-mount antibody staining on T5MO and CMO embryos for tropomyosin. Consistent with the RT-PCR analysis, we observed a delay in the expression of tropomyosin in T5MO embryos in comparison with CMO embryos (Fig. 4B–I). As further confirmation that the timing of differentiation is altered in response to TBX5 depletion in vivo, we injected embryos carrying the cardiac actin:GFP transgene (Latinkic et al., 2002) with T5MO or CMO and monitored skeletal muscle and heart development in living staged-matched embryos (Fig. 4J–Q). Although we could not detect any alteration in the timing of GFP expression in skeletal muscle (data not shown), we observed a consistent and significant delay in the time at which GFP was first expressed in the hearts of the T5MO embryos. Collectively, these results suggest that control of the cardiac cell cycle by TBX5 leads to an alteration in the timing of the cardiac program.

TBX5 depletion leads to abnormal sarcomere formation

To determine if cardiomyocyte differentiation in T5MO hearts occurs in all cardiomyocytes or only in a subset of cells, we analyzed cardiomyocyte differentiation by immunohistochemistry on cross-sections of CMO- and T5MO-derived tissues (Fig. 5A–H). Results clearly showed that by stage 37 we could detect staining of troponin T (cTnT), MHC and Tmy throughout the myocardium of control and T5MO hearts, suggesting that all cardiomyocytes in T5MO undergo terminal differentiation.

To examine sarcomere and cytoskeletal structure in greater detail, we double-labeled hearts from CMO and T5MO embryos with the cardiomyocyte marker Tmy and antibodies that recognize either components of the cardiac extracellular matrix (ECM), fibronectin and fibrillin, or mark cardiomyocyte polarity, β-catenin (Fig. 5I–N) (Trinh and Stainier, 2004). This analysis revealed that TBX5 depletion led to hearts with defects in both sarcomere and ECM development. By contrast to CMO-derived hearts, which form sarcomeres throughout the myocardium, T5MO hearts form sarcomeres only in cells adjacent to the lumen of heart (Fig. 5G,H,O,P). Moreover, the sarcomeres that form often lacked A- and Z-bands and frequently failed to give rise to myofibrils (Fig. 5O,P). These alterations in cardiomyocyte differentiation coincided with elevated fibronectin deposition, particularly within the dorsal portion of the T5MO where the heart remains unfused (Fig. 5I,J) and an increase in both fibronectin and fibrillin deposition on the walls of the heart chamber (Fig. 5I–L). However, we could detect no alteration in β-catenin expression (Fig. 5M,N). We also noted that at this stage it appeared that the majority of β-catenin was associated with the myocardial membranes, with little to no β-catenin in the cytoplasm or nucleus. Taken together, these data suggest that alteration in cardiac cell cycle progression due to the depletion of TBX5 leads to abnormal cardiomyocyte and ECM maturation.

To confirm these structural alterations in TBX5-depleted heart tissue, we carried out ultrastructural analyses on CMO and T5MO hearts by high magnification confocal microscopy (Fig. 5O,P) and transmission electron microscopy (TEM) (Fig. 5Q–V). High magnification imaging of cardiac tissue immunostained with Tmy revealed that the cardiac cells in CMO embryos formed myofibrils that were distributed throughout the myocardium (Fig. 5O). By

contrast, the myofibrils in T5MO cardiac cells were poorly organized and formed only adjacent to the cardiac lumen (Fig. 5P).

Consistent with immunostaining for cardiac muscle, we found in transverse TEM sections of CMO embryos that cardiac muscle bundles were located throughout the myocardium, positioned in both longitudinal and concentric arrays (Fig. 5Q). By contrast, T5MO hearts showed far fewer sarcomeres than controls, and the cells bordering the pericardial space of T5MO hearts, in contrast with those bordering the heart lumen, completely lacked bundles of cardiac muscle fibers (Fig. 5R,S,V). Moreover, the sarcomeres that formed frequently lacked distinct A- and Z-bands, and the A-and Z-bands that were present were poorly defined (Fig. 5T,U). This does not appear to represent simply a delay in myofibril formation, as during normal development myofibrils form throughout the myocardium and do not show any temporal differences in differentiation between distal and proximal cardiomyocytes (Kolker et al., 2000) (Y. Langdon and F.L.C., unpublished).

Taken together, our immunohistochemistry and ultrastructural analysis suggest that the G_1/S-phase delay or arrest in TBX5-depleted embryos results in an alteration in the timing of the cardiac program, leading to asymmetric and aberrant sarcomere formation. Moreover, these results imply that TBX5 is not required for the onset of cardiac differentiation but is required to either establish or maintain cardiomyocyte and cytoskeletal architecture.

TBX5 is both necessary and sufficient for the progression of the embryonic cardiac cell cycle

Our analysis of T5MO embryos shows a requirement for TBX5 in embryonic cell cycle progression and a role in controlling the correct timing of cardiac differentiation. To determine if TBX5 is sufficient to regulate these two processes, we misexpressed *Tbx5* in early *Xenopus* embryos (Fig. 6). Although injection of *Tbx5* RNA at the single cell stage caused *Tbx5* misexpression throughout the embryo, phenotypic abnormalities were restricted to the anterior and cardiac regions of the early tadpole (Fig. 6A–C; data not shown). To further analyze these defects, we carried out whole-mount in-situ hybridization analyses on uninjected control and *Tbx5*-injected embryos (Fig. 6D–G; data not shown). Similar to results from TBX5 depletion, this analysis shows that *Tbx5* misexpression did not block cardiac commitment, migration or terminal differentiation, as judged by *Nkx2.5* and myosin light chain (MLC) expression (Fig. 6D–G).

To test if *Tbx5* cardiac defects are associated with alteration in the cardiac cell cycle, we serial-sectioned embryos at stage 37 and stained with the mitotic marker anti-pH3. We found that *Tbx5* misexpression had the opposite effect of depleting TBX5, leading to a two-fold increase in the cardiac cell mitotic index (Fig. 6H).

To ensure that the increase in mitotic index is tissue-specific, we calculated the mitotic index in the ventricular zone of the neural tube in the same sections as those containing the heart tissue, i.e. sections that correspond exactly to the same point along the anterior-posterior axis. We could not detect a difference between control or *Tbx5*-misexpressing-derived neural tissue. Therefore, the increase in mitotic index within appears to be cardiac-specific.

To test whether TBX5 is also sufficient for the correct timing of cardiac differentiation, we again collected stage-matched embryos from stage 10 to stage 38 and carried out RT-PCR with primers specific for the early cardiac marker *Nkx2.5*, and for markers of cardiac and skeletal muscle differentiation (Fig. 6J). Consistent with our results for the in-situ hybridization experiment, we found no alteration in *Nkx2.5* expression in *Tbx5*-injected embryos. Results for the cardiac differentiation markers showed the exact opposite of those for TBX5 depletion: *Tbx5*-injected embryos initially expressed Troponin and MHC at later stages than controls (stage 38 in *Tbx*-injected embryos versus stage 28 in control embryos) but turned on Tmy at

earlier stages (stage 16 in *Tbx5*-injected embryos versus 22 in control embryos). As we did not observe any changes in the timing at which skeletal muscle markers were expressed, the alteration in timing of expression again appeared to be specific to cardiac tissue. Collectively, these studies strongly suggest that TBX5 is both necessary and sufficient to regulate progression of the embryonic cardiac cell cycle and the timing of the cardiac program.

DISCUSSION

Despite the crucial importance of understanding cell cycle control for both normal development and disease, relatively little is known about the proteins that regulate these processes in the embryonic heart. We demonstrate that that TBX5 is both necessary and sufficient to control embryonic cardiac cell proliferation and cell number by regulating the length of the embryonic cardiac cell cycle. Our results show that depletion of TBX5 led to a delay or arrest in G_1- or S-phase, as judged by the upregulation of the G_1/S-phase-associated proteins and the concomitant decrease in the cardiac mitotic index. If the arrest was occurring at the S/G2 transition, Cdc6 and Cyclin E2 levels should be equivalent between T5MO and control heart tissue. Moreover, cyclin A2 and Cdk1 should be significantly elevated in the T5MO hearts. As our results clearly show that the level of neither protein was altered in the T5MO tissue relative to the control, our data strongly suggest that the arrest does not occur at S/G2 but at the G_1/S-phase transition. Because cyclins E and A are thought to be expressed sequentially during S-phase, and because we observed an increase in cyclin E2 but not in cyclin A2, our results predict that S-phase arrest in TBX5-depleted embryos would occur at the G_1/S-phase transition or in early S-phase. Based on these findings, we propose that depleting TBX5 results in a prolonged or blocked early S-phase, resulting in fewer rounds of proliferation, in turn leading to the reduced cardiac cell number we observed in T5MO embryos (Fig. 7).

Past studies have implied that the myocardium undergoes a fixed number of intrinsically determined cell divisions before entering a postmitotic state and undergoing cardiac differentiation (Burton et al., 1999). It appears that TBX5 interferes with this autonomous program by forcing cells into a prolonged or arrested S-phase and thus differentiating without undergoing a predetermined number of cell divisions. As in the TBX5-depleted embryos and embryos misexpressing *Tbx5* the timing of the cardiac differentiation program was altered compared to controls, our results imply that proper S-phase progression, and possibly a determined number of divisions, are required for the proper timing, but not the initiation, of heart differentiation. Our results further imply that a reduced number of cardiac divisions leads to a delay in the expression of some markers of terminal differentiation, including cardiac actin and tropomyosin. By contrast, we note that troponin and MHC were expressed earlier in T5MO cardiac tissue and later in hearts from embryos misexpressing *Tbx5*, suggesting that these markers are controlled in a different fashion from other cardiac differentiation markers.

TBX5 and embryonic cardiac cell cycle control

Like other members of the T-box gene family, TBX5 has been shown to function as a transcription factor; TBX5 is localized to the nucleus, it binds to DNA in a sequence specific fashion and it regulates the transcriptional level of its target genes. Our present studies suggest that at least one of the targets of TBX5 either directly or indirectly functions to control the progression of the embryonic cardiac cell cycle. What are the mechanisms by which this may occur? One possibility is that TBX5 could function to induce the expression of a growth factor, for example EGF or FGF, which in turn is required for cell cycle progression. In the absence of this growth factor the cell cycle may not proceed through to the completion of G_1 (Fig. 7). Alternatively, TBX5 may function to regulate the expression of a key component of the pre-replication complex. In the absence of this key component the pre-replication complex may

not assemble or may not load onto the origins of replication (ORCs), thus blocking DNA synthesis and hence cell cycle progression (Fig. 7).

Cell cycle progression through G_1/S is regulated by members of the E2F family of transcription factors, the function of which is governed through their interaction with the retinoblastoma protein (Rb). In its hypophosphorylated state, Rb interacts with E2F, inhibiting its transcriptional activation activity. Upon Rb phosphorylation, the Rb-E2F interaction is disrupted and E2F is released and able to activate its downstream genes required for S-phase entry (Cobrinik, 2005). Thus, one function of TBX5 may be to indirectly regulate the state of Rb phosphorylation. Finally, TBX5 may function to negatively regulate general cell cycle inhibitors such as $p27^{Xic}$ (Fig. 7). Our data cannot distinguish between these possibilities, and the exact molecular pathway by TBX5 functions awaits the identification of TBX5 cell cycle target genes.

Tbx5 misexpression leads to cardiac-specific defects

We have shown that misexpression of *Tbx5* leads to cardiac defects in vivo. This effect appeared to be specific, as misexpression of other T-box-containing genes does not give a similar phenotype (Showell et al., 2004). These results demonstrate that the absolute levels of TBX5 are crucial for normal heart development in vivo; increased levels of TBX5 results in abnormal heart formation and reduction of TBX5 levels by just half leads to HOS. Interestingly, the defects we observed with *Tbx5* misexpression were specific to the anterior and cardiac regions of the embryo, with the cardiac defects resembling those seen with *Nkx2.5* misexpression (Cleaver, 1996; Tonissen et al., 1994). The similarity between the *Tbx5* and *Nkx2.5* overexpression phenotypes raises the possibility that the misexpression phenotype we observed in TBX5 was due to an upregulation of *Nkx2.5*. However, a number of our findings would suggest that this is not the case. Most crucially, we have conducted in-situ hybridization as well as RT-PCR to examine *Nkx2.5* expression in embryos misexpressing *Tbx5* during early stages of early heart development. We have shown that misexpression of *Tbx5* did not lead to altered spatial or temporal patterns or levels of *Nkx2.5* expression at any stage. These results are consistent with our previously published results showing that the loss of TBX5 has no effect on the temporal or spatial expression of *Nkx2.5* (Brown et al., 2005). Therefore, misexpression of *Tbx5* appears to alter the cardiac mitotic index in an *Nkx2.5*-independent fashion.

Our finding that *Tbx5* misexpression resulted in an increased mitotic index differs from two previous studies implying that *Tbx5* expression inhibits cell growth or survival (Hatcher et al., 2001; Liberatore et al., 2000). However, in these reports *Tbx5* is misexpressed after expression of endogenous *Tbx5* is initiated and, consequently, after the commitment and differentiation of the heart have taken place. Thus, it may be possible that TBX5 has two opposing functions during development: an early function in regulating cardiac cell cycle progression and a late function instructing cardiac cells to undergo cell cycle arrest. Alternatively, overexpression of TBX5 may lead to it binding and activating non-endogenous targets, in particular those of other T-box genes, such as TBX2, TBX3, TBX18 or TBX20 (Harvey, 2002; Stennard and Harvey, 2005), which may function during the later stages of cardiogenesis to regulate cell cycle exit.

Holt-Oram syndrome

HOS is an autosomal dominant disease arising from haploinsufficiency of TBX5 and is associated with conduction-system abnormalities, secundum atrial defect and ventricular septal defects (Basson et al., 1997; Li et al., 1997; Newbury-Ecob et al., 1996). Consistent with these phenotypic abnormalities, *Tbx5* has been shown to be expressed in the atrial wall, the atrial septa and the atrial aspects of the atrioventricular valves (Hatcher et al., 2000). The role of TBX5 in heart development is further emphasized by the observation that mice heterozygous for mutations in *Tbx5* display many of the abnormalities described in HOS patients (Bruneau

et al., 2001). However, the cellular basis for defects in HOS remains unclear. Our results would suggest that TBX5 functions to regulate the length of the G_1/S cycle within the subset of heart tissues in which it is expressed. In HOS, G_1/S-phase would be significantly lengthened or blocked, leading to a decrease in cell cycle progression and defects in cell proliferation due to a successive decrease in the number of cell divisions, and ultimately programmed cell death in the affected regions.

Acknowledgements

This work is supported by grants to F.L.C. from the NIH/NHLBI, RO1 HL075256 and R21HL083965, and by an award from the UNC Medical Alumni Association. S.C.G. is a trainee in the Integrative Vascular Biology program supported by T32HL69768 from the National Institutes of Health. The antibodies against tropomyosin and cardiac troponin (developed by J.-C. Lin), and fibrillin (developed by C. D. Little) were obtained from the Developmental Studies Hybridoma Bank, developed under the auspices of the NICHD and maintained by the University of Iowa, Department of Biological Sciences, Iowa City, IA 52242. We are grateful to Drs Martine Coué for the Cdt1 and Cdc6 antibodies, William Marzluff for the SLBP antibody, Timothy Hunt for the cyclin B2 antibody and Timothy Mohun for the cardiac actin-GFP transgenic *Xenopus* line. We thank Victoria Madden and Elena Davis of the UNC Microscopy Services Laboratory for assistance with TEM. We thank Dr Olav Binder for the in-situ hybridization images used in Fig. 6. We acknowledge Robert Duronio for his time, patience and help with this work. We also thank Larysa Pevny, Elizabeth Mandel and Mark Majesky for critical reading of the manuscript and helpful suggestions.

References

Agius E, Oelgeschlager M, Wessely O, Kemp C, De Robertis EM. Endodermal Nodal-related signals and mesoderm induction in Xenopus. Development 2000;127:1173–1183. [PubMed: 10683171]

Anversa P, Kajstura J. Ventricular myocytes are not terminally differentiated in the adult mammalian heart. Circ Res 1998;83:1–14. [PubMed: 9670913]

Basson CT, Bachinsky DR, Lin RC, Levi T, Elkins JA, Soults J, Grayzel D, Kroumpouzou E, Traill TA, Leblanc-Straceski J, et al. Mutations in human TBX5 [corrected] cause limb and cardiac malformation in Holt-Oram syndrome. Nat Genet 1997;15:30–35. [PubMed: 8988165]

Basson CT, Huang T, Lin RC, Bachinsky DR, Weremowicz S, Vaglio A, Bruzzone R, Quadrelli R, Lerone M, Romeo G, et al. Different TBX5 interactions in heart and limb defined by Holt-Oram syndrome mutations. Proc Natl Acad Sci USA 1999;96:2919–2924. [PubMed: 10077612]

Benson DW, Basson CT, MacRae CA. New understandings in the genetics of congenital heart disease. Curr Opin Pediatr 1996;8:505–511. [PubMed: 8946132]

Brown DD, Martz SN, Binder O, Goetz SC, Price BM, Smith JC, Conlon FL. Tbx5 and Tbx20 act synergistically to control vertebrate heart morphogenesis. Development 2005;132:553–563. [PubMed: 15634698]

Bruneau BG, Nemer G, Schmitt JP, Charron F, Robitaille L, Caron S, Conner DA, Gessler M, Nemer M, Seidman CE, et al. A murine model of Holt-Oram syndrome defines roles of the T-box transcription factor Tbx5 in cardiogenesis and disease. Cell 2001;106:709–721. [PubMed: 11572777]

Burton PB, Raff MC, Kerr P, Yacoub MH, Barton PJ. An intrinsic timer that controls cell-cycle withdrawal in cultured cardiac myocytes. Dev Biol 1999;216:659–670. [PubMed: 10642800]

Charbonnier F, Gaspera BD, Armand AS, Van der Laarse WJ, Launay T, Becker C, Gallien CL, Chanoine C. Two myogenin-related genes are differentially expressed in Xenopus laevis myogenesis and differ in their ability to transactivate muscle structural genes. J Biol Chem 2002;277:1139–1147. [PubMed: 11684685]

Cleaver OB, Patterson KD, Krieg PA. Overexpressoin of the *tinman*-related genes XNkx-2.5 and XNkx-2.3 in *Xenopus* embryos results in myocardial hyperplasia. Development 1996;122:3549–3556. [PubMed: 8951070]

Cobrinik D. Pocket proteins and cell cycle control. Oncogene 2005;24:2796–2809. [PubMed: 15838516]

Fishman MC, Chien KR. Fashioning the vertebrate heart: earliest embryonic decisions. Development 1997;124:2099–2117. [PubMed: 9187138]

Garrity DM, Childs S, Fishman MC. The heartstrings mutation in zebrafish causes heart/fin Tbx5 deficiency syndrome. Development 2002;129:4635–4645. [PubMed: 12223419]

Harland RM. In situ hybridization: an improved whole-mount method for Xenopus embryos. Methods Cell Biol 1991;36:685–695. [PubMed: 1811161]

Harvey RP. Patterning the vertebrate heart. Nat Rev Genet 2002;3:544–556. [PubMed: 12094232]

Hatcher CJ, Goldstein MM, Mah CS, Delia CS, Basson CT. Identification and localization of TBX5 transcription factor during human cardiac morphogenesis. Dev Dyn 2000;219:90–95. [PubMed: 10974675]

Hatcher CJ, Kim MS, Mah CS, Goldstein MM, Wong B, Mikawa T, Basson CT. TBX5 transcription factor regulates cell proliferation during cardiogenesis. Dev Biol 2001;230:177–188. [PubMed: 11161571]

Hiroi Y, Kudoh S, Monzen K, Ikeda Y, Yazaki Y, Nagai R, Komuro I. Tbx5 associates with Nkx2-5 and synergistically promotes cardiomyocyte differentiation. Nat Genet 2001;28:276–280. [PubMed: 11431700]

Hochegger H, Klotzbucher A, Kirk J, Howell M, le Guellec K, Fletcher K, Duncan T, Sohail M, Hunt T. New B-type cyclin synthesis is required between meiosis I and II during Xenopus oocyte maturation. Development 2001;128:3795–3807. [PubMed: 11585805]

Hopwood ND, Pluck A, Gurdon JB. MyoD expression in the forming somites is an early response to mesoderm induction in Xenopus embryos. EMBO J 1989;8:3409–3417. [PubMed: 2555164]

Horb ME, Thomsen GH. Tbx5 is essential for heart development. Development 1999;126:1739–1751. [PubMed: 10079235]

Kajstura J, Leri A, Castaldo C, Nadal-Ginard B, Anversa P. Myocyte growth in the failing heart. Surg Clin North Am 2004;84:161–177. [PubMed: 15053188]

Kolker SJ, Tajchman U, Weeks DL. Confocal imaging of early heart development in Xenopus laevis. Dev Biol 2000;218:64–73. [PubMed: 10644411]

Latinkic BV, Cooper B, Towers N, Sparrow D, Kotecha S, Mohun TJ. Distinct enhancers regulate skeletal and cardiac muscle-specific expression programs of the cardiac alpha-actin gene in Xenopus embryos. Dev Biol 2002;245:57–70. [PubMed: 11969255]

Li QY, Newbury-Ecob RA, Terrett JA, Wilson DI, Curtis AR, Yi CH, Gebuhr T, Bullen PJ, Robson SC, Strachan T, et al. Holt-Oram syndrome is caused by mutations in TBX5, a member of the Brachyury (T) gene family. Nat Genet 1997;15:21–29. [PubMed: 8988164]

Liberatore CM, Searcy-Schrick RD, Yutzey KE. Ventricular expression of tbx5 inhibits normal heart chamber development. Dev Biol 2000;223:169–180. [PubMed: 10864469]

MacLellan WR, Schneider MD. Genetic dissection of cardiac growth control pathways. Annu Rev Physiol 2000;62:289–319. [PubMed: 10845093]

Mandel EM, Callis T, Wang DZ, Conlon FL. Transcriptional mechanisms of congenital heart disease. Drug Discov Today Dis Mech 2005;2:33–38.

McKinsey TA, Zhang CL, Olson EN. MEF2: a calcium-dependent regulator of cell division, differentiation and death. Trends Biochem Sci 2002;27:40–47. [PubMed: 11796223]

Mikawa T, Borisov A, Brown AM, Fischman DA. Clonal analysis of cardiac morphogenesis in the chicken embryo using a replication-defective retrovirus: I. Formation of the ventricular myocardium. Dev Dyn 1992a;193:11–23. [PubMed: 1540702]

Mikawa T, Cohen-Gould L, Fischman DA. Clonal analysis of cardiac morphogenesis in the chicken embryo using a replication-defective retrovirus. III: polyclonal origin of adjacent ventricular myocytes. Dev Dyn 1992b;195:133–141. [PubMed: 1297456]

Mohun T, Orford R, Shang C. The origins of cardiac tissue in the amphibian, Xenopus laevis. Trends Cardiovasc Med 2003;13:244–248. [PubMed: 12922021]

Mohun TJ, Leong LM, Weninger WJ, Sparrow DB. The morphology of heart development in Xenopus laevis. Dev Biol 2000;218:74–88. [PubMed: 10644412]

Newbury-Ecob RA, Leanage R, Raeburn JA, Young ID. Holt-Oram syndrome: a clinical genetic study. J Med Genet 1996;33:300–307. [PubMed: 8730285]

Nieuwkoop PD. The “organization centre”. 3 Segregation and pattern formation in morphogenetic fields. Acta Biotheor 1967;17:178–194. [PubMed: 4967351]

Olson EN, Schneider MD. Sizing up the heart: development redux in disease. Genes Dev 2003;17:1937–1956. [PubMed: 12893779]

Papaioannou VE, Silver LM. The T-box gene family. BioEssays 1998;20:9–19. [PubMed: 9504043]

Pasumarthi KB, Field LJ. Cardiomyocyte cell cycle regulation. Circ Res 2002;90:1044–1054. [PubMed: 12039793]

Plageman TF Jr, Yutzey KE. Differential expression and function of Tbx5 and Tbx20 in cardiac development. J Biol Chem 2004;279:19026–19034. [PubMed: 14978031]

Rybkin II, Markham DW, Yan Z, Bassel-Duby R, Williams RS, Olson EN. Conditional expression of SV40 T-antigen in mouse cardiomyocytes facilitates an inducible switch from proliferation to differentiation. J Biol Chem 2003;278:15927–15934. [PubMed: 12590133]

Showell C, Binder O, Conlon FL. T-box genes in early embryogenesis. Dev Dyn 2004;229:201–218. [PubMed: 14699590]

Small EM, Krieg PA. Expression of atrial natriuretic factor (ANF) during Xenopus cardiac development. Dev Genes Evol 2000;210:638–640. [PubMed: 11151301]

Soonpaa MH, Field LJ. Survey of studies examining mammalian cardiomyocyte DNA synthesis. Circ Res 1998;83:15–26. [PubMed: 9670914]

Stennard FA, Harvey RP. T-box transcription factors and their roles in regulatory hierarchies in the developing heart. Development 2005;132:4897–4910. [PubMed: 16258075]

Tonissen KF, Drysdale TA, Lints TJ, Harvey RP, Krieg PA. XNkx-2.5, a Xenopus gene related to Nkx-2.5 and tinman: evidence for a conserved role in cardiac development. Dev Biol 1994;162:325–328. [PubMed: 7545912]

Trinh LA, Stainier DY. Fibronectin regulates epithelial organization during myocardial migration in zebrafish. Dev Cell 2004;6:371–382. [PubMed: 15030760]

Vernon AE, Philpott A. The developmental expression of cell cycle regulators in Xenopus laevis. Gene Expr Patterns 2003;3:179–192. [PubMed: 12711547]

Wang ZF, Ingledue TC, Dominski Z, Sanchez R, Marzluff WF. Two Xenopus proteins that bind the 3′ end of histone mRNA: implications for translational control of histone synthesis during oogenesis. Mol Cell Biol 1999;19:835–845. [PubMed: 9858606]

Whitmire E, Khan B, Coue M. Cdc6 synthesis regulates replication competence in Xenopus oocytes. Nature 2002;419:722–725. [PubMed: 12384699]

Wilson PA, Hemmati-Brivanlou A. Induction of epidermis and inhibition of neural fate by Bmp-4. Nature 1995;376:331–333. [PubMed: 7630398]

Wilson V, Conlon FL. The T-box family. Genome Biol 2002;3:REVIEWS3008. [PubMed: 12093383]

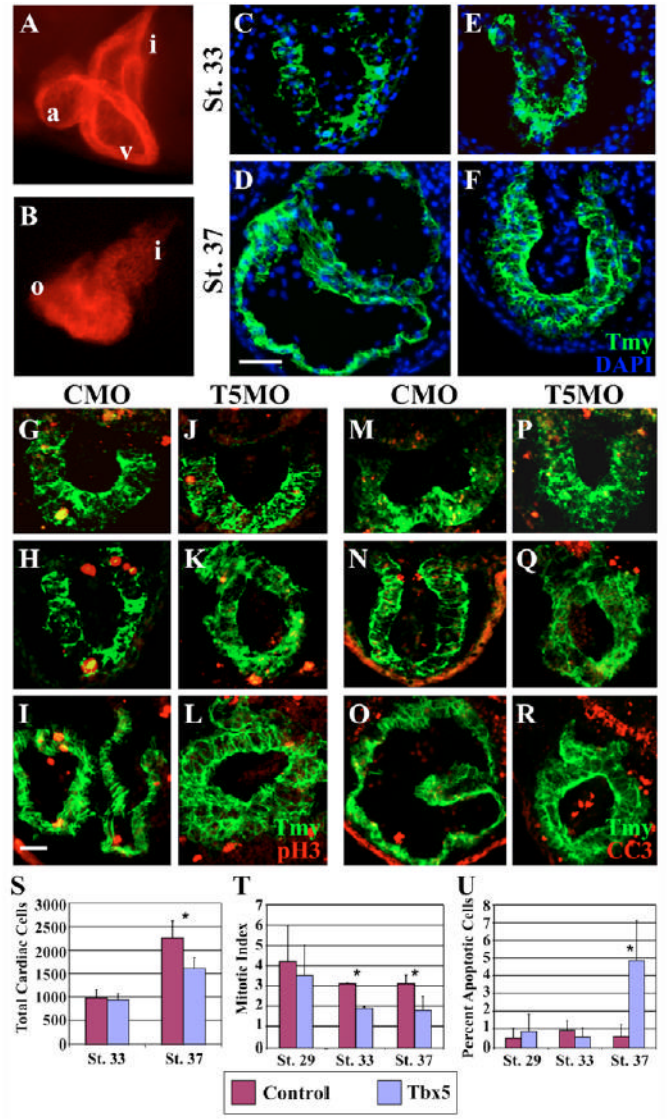

Fig. 1. TBX5 is required for cardiac proliferation

Whole-mount antibody staining with tropomyosin (Tmy) of stage 37 (**A**) control morpholino (CMO) or (**B**) TBX5 morpholino (T5MO) embryos. Transverse heart sections through (C,E) stage 33 and (D,F) stage 37 embryos stained with Tmy, to mark cardiac tissue, and DAPI, to mark cell nuclei; (**C**,**D**) CMO-derived tissue; (**E**,**F**) T5MO-derived tissue. (**G–L**) Examples of proliferating cardiac cells in transverse heart sections from (G–I) CMO and (J–L) T5MO embryos sectioned through the cardiac region at stages 29, 33 and 37, as indicated. Proliferating cardiomyocytes are identified as those positive for Tmy (myofibrilis shown as green) and anti-phosphohistone H3 (pH3; localized to the nucleus and shown in red). (**M**–**R**) Examples of cardiac cells undergoing apoptosis in transverse heart sections from (M–O) CMO and (P–R) T5MO embryos at stages 29, 33 and 37, as indicated. Apoptotic cardiomyocytes are identified as those positive for Tmy (myofibrilis shown as green) and anti-cleaved caspase 3 (CC3; localized to the nucleus and shown in red). Quantification of results from (**S**) total cardiomyocyte cell numbers, (**T**) mitotic index, and (**U**) programmed cell death. In all cases, bars represent the average of at least three embryos: CMO, red bar and T5MO, blue bar. Error bars denote the standard deviation, and * denotes a statistically significant difference (at $P<0.05$) between CMO and T5MO embryos at a given stage. Results are derived from a single

set of experiments, all experiments being repeated at least once with an independent batch of embryos. Scale bars: 50 μm. a, atrium; i, inflow tract; o, outflow tract; v, ventricle.

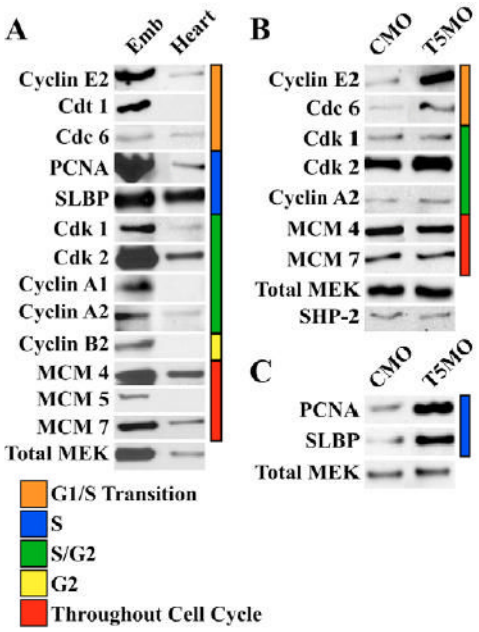

Fig. 2. TBX5 depletion results in dramatic upregulation of proteins associated with G_1/S-phase within the heart

(**A**) Expression profile of cell-cycle associated proteins, as determined by western blot analysis performed using lysate from either whole stage 33 embryos (emb), or corresponding heart tissue (heart). (**B**) Relative differences in embryonic cardiac CDK and cyclin proteins between CMO- and T5MO-derived heart tissue (stage 33). Note increased levels of Cyclin E2, CDC6, CDK2. (**C**) Relative differences in embryonic cardiac S-phase associated proteins SLBP and PCNA between CMO- and T5MO-derived heart tissue (stage 33). Colored bars denote the stage of the cell cycle at which the proteins are expressed, as indicated in the key.

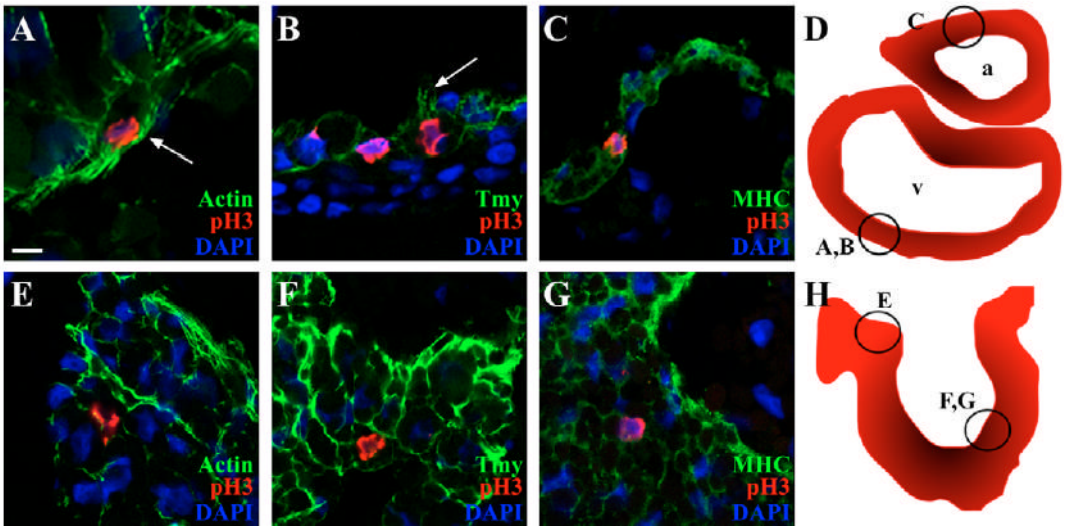

Fig. 3. Terminally differentiated cardiomyocytes retain the capacity to undergo cell division

Transverse sections of (**A–C**) CMO or (**E–G**) T5MO heart tissues at stage 37, showing cells coexpressing pH3 (red), DAPI (blue) and either (A,E) actin, (B,F) Tmy or (C,G) MHC (all shown in green). (**D**) Schematic of a CMO heart displaying the relative positions of each panel. A and B were imaged from an area corresponding with 'A,B'; C was imaged from a region corresponding with 'C'. (**H**) Schematic of a T5MO heart displaying the relative positions of each panel. E corresponds with 'E'; F and G correspond with 'F,G'. White arrows denote sarcomeric bundles. Scale bar: 10 μm. a, atrium; v, ventricle.

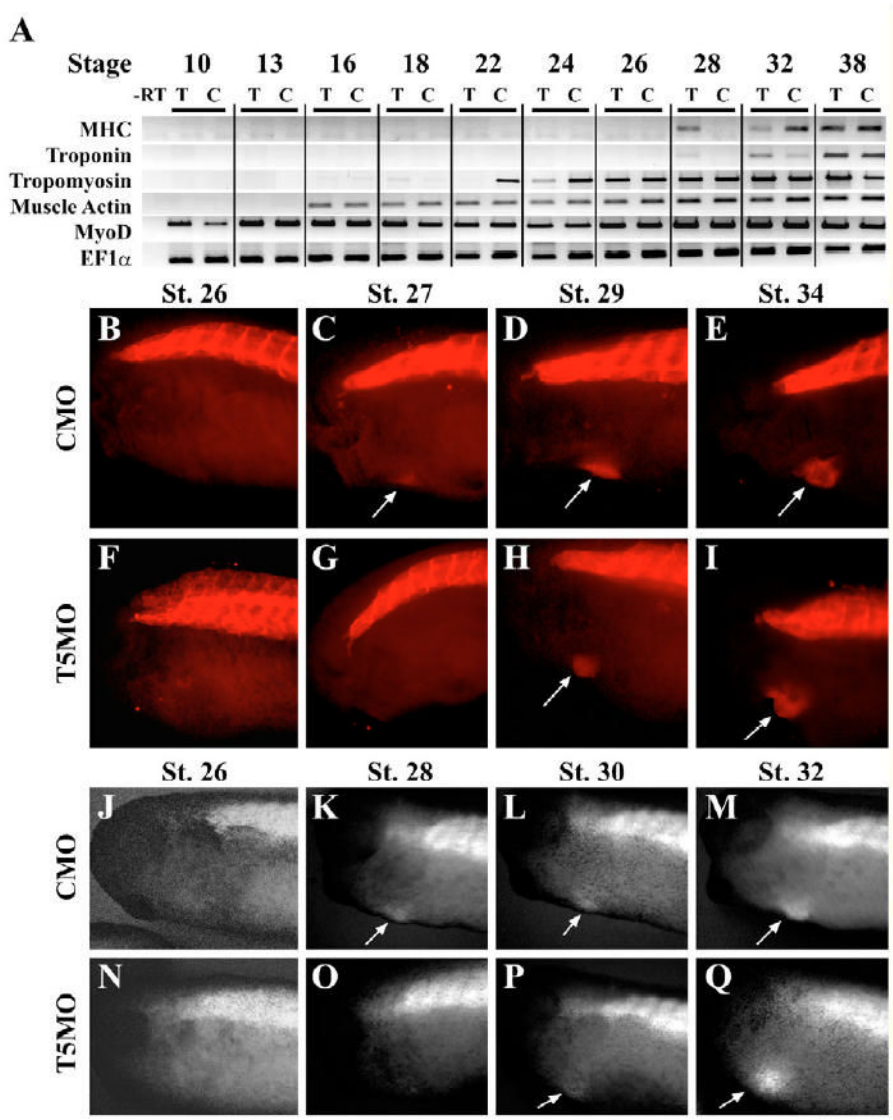

Fig. 4. The timing of the cardiac differentiation program is altered in TBX5-depleted embryos

(**A**) RT-PCR analysis of the expression of heart-specific isoforms of MHC, troponin and tropomyosin; and skeletal muscle-specific genes MyoD and muscle actin, throughout early and mid-tadpole stages of development in CMO ('C') and T5MO ('T') stage-matched embryos. All samples are derived from a single batch of eggs, and identical results were achieved in at least two independent sets of experiments for each marker. EF1-Alpha was used as a loading control for all RT-PCR reactions. (**B–I**) Images depicting embryos injected with (B–E) CMO, or (F–I) T5MO and immunostained for Tmy, showing delayed expression of Tmy in the hearts of T5MO embryos. Shown are representative sibling embryos imaged at the indicated stages. White arrows denote expression of Tmy within the heart. (**J–Q**) Images of living cardiac actin:GFP transgenic embryos, showing a delay in the onset of cardiac actin expression in the heart. Representative sibling embryos obtained from a single batch of embryos were injected with (J–M) CMO or (N–Q) T5MO and imaged at the indicated stages. Shown is a representative pair of embryos, while identical results were observed in over 50 embryos. White arrows denote expression of GFP within the heart field.

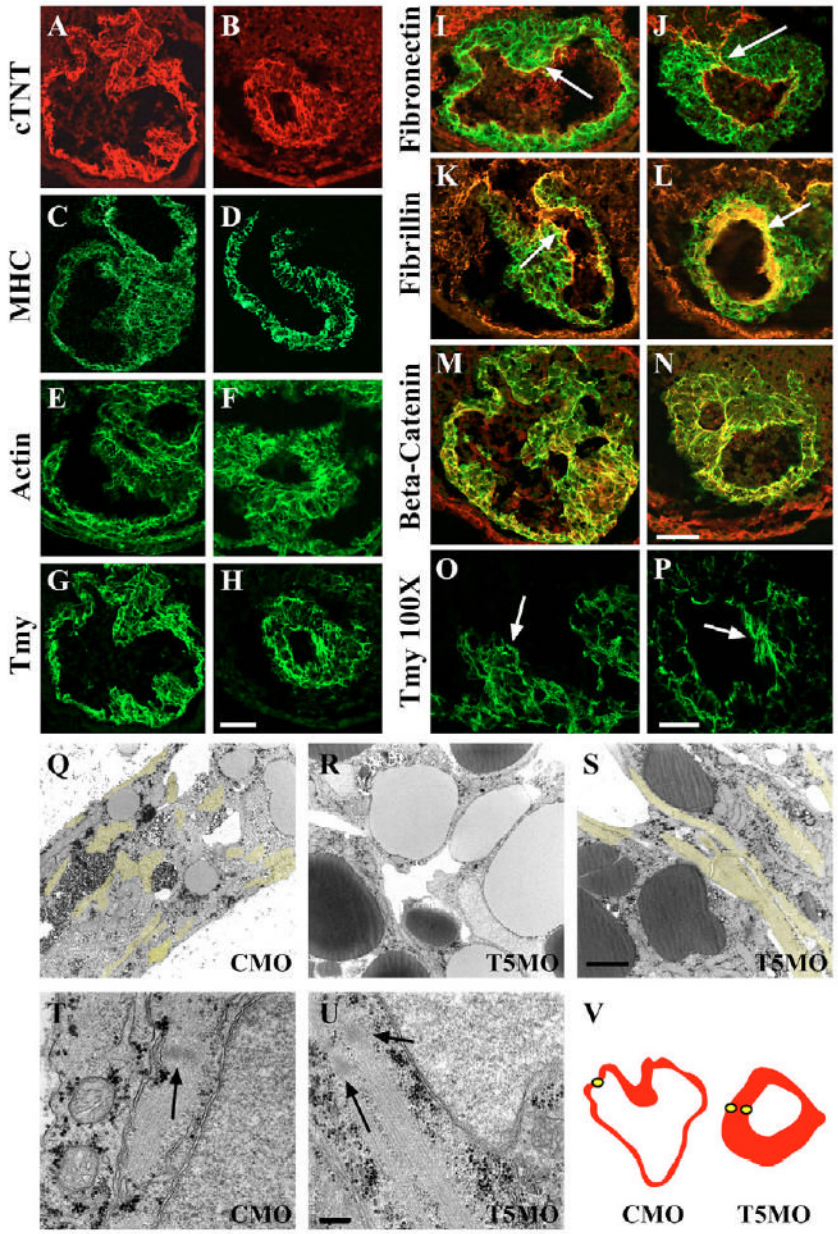

Fig. 5. TBX5 depletion leads to a disruption in cardiac myofibril structure

Cardiomyocyte structure in transverse sections through the hearts of (A,C,E,G) CMO or (B,D,F,H) T5MO stage 37 embryos, as detected by immunostaining for (**A**,**B**) cardiac troponin T (cTNT), (**C**,**D**) MHC, (**E**,**F**) actin or (**G**,**H**) Tmy. (I,K,M) Stage 37 CMO or (J,L,N) T5MO embryos double-immunostained for tropomyosin (green) and (**I**,**J**) fibronectin, (**K**,**L**) fibrillin or (**M**,**N**) β-catenin, all shown in red. Note increase in fibrillin staining on the walls of the chamber of T5MO hearts relative to CMO (compare panel K to L, white arrows) and ectopic expression of fibronectin, shown by white arrow, in the dorsal portion of the heart in panel J relative to panel I. (**O**,**P**) High magnification confocal images of hearts from (O) CMO or (P) T5MO stage 37 embryos. Note that formation of organized cardiac muscle bundles in T5MO hearts is limited to a single cluster adjacent to the cardiac lumen. (**Q**–**S**) Representative transmission electron micrographs of transverse images of stage 37 embryos taken from (Q)

CMO cardiac tissue or (R) T5MO cardiac tissue adjacent to the pericardial cavity and (S) T5MO cardiac tissue adjacent to the cardiac lumen. Cardiac muscle fibrils are shown pseudo-colored in yellow. Note that sarcomeres in T5MO hearts can only be identified adjacent to the cardiac lumen (compare R with S) and only found in concentric arrays. By contrast, CMO-derived hearts show both longitudinal and concentric arrays (compare Q with S). High-magnification TEM images reveal the ultrastructures of (**T**) CMO and (**U**) T5MO cardiac sarcomeres. Arrows denote A-bands. Note the smaller, non-continuous A-bands in the T5MO-derived sarcomeres (U). (**V**) Traces of the heart sections from CMO and T5MO embryos imaged by TEM are depicted schematically. Yellow circles represent the location of TEM imaging. Scale bars: 50 μm in A–N; 2 μm in Q–S; 0.2 μm in T,U.

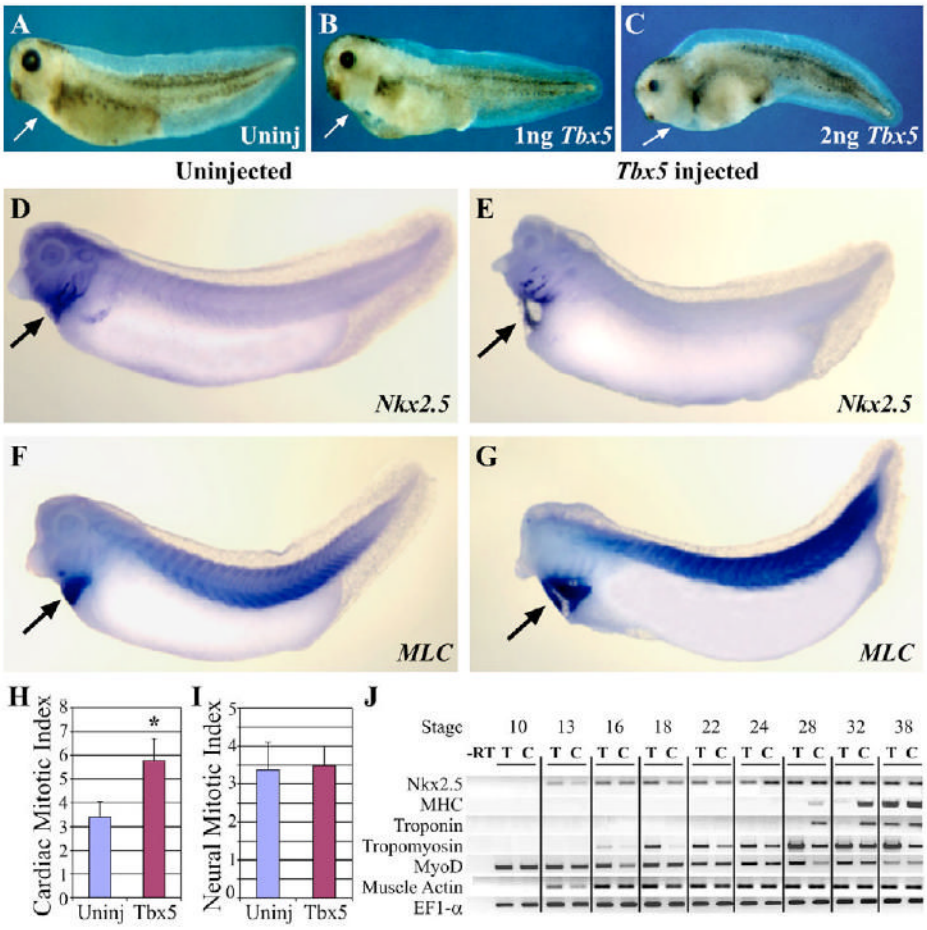

Fig. 6. *Tbx5* misexpression leads to changes in cardiac proliferation and morphology

The overall morphology of stage 40 (**A**) uninjected embryos or (**B**,**C**) embryos injected with increasing amounts of *Tbx5* RNA, as indicated. Arrows denote the location of the heart. (**D**–**G**) Whole-mount in-situ hybridization showing expression of (D,E) *Nkx2.5* and (F,G) myosin light chain (MLC) in (D,F) uninjected stage 37 embryos and (E,G) stage-matched embryos injected with 1 ng of *Tbx5* RNA. (**H**) *Tbx5* misexpression leads to an increase in the cardiac mitotic index at stage 37. Mitotic index was calculated as the percentage of cardiac cells labeled with pH3. The data represents the mean of at least three different embryos. Error bars denote the standard deviation, and * denotes a statistically significant difference between *Tbx5*-injected and control embryos (at $P<0.05$). (**I**) Mitotic index for sections of the neural tube corresponding to the same position as the heart along the anterior-posterior axis. The data represents the mean mitotic index of four different embryos per condition, with four sections analyzed per embryo. Error bars denote the standard deviation. (**J**) *Tbx5* misexpression leads to an alteration in the timing and order of the cardiac differentiation program. RT-PCR analysis of the expression of *Nkx2.5* as well as heart-specific isoforms of MHC, troponin and tropomyosin, and skeletal-muscle-specific genes, MyoD and muscle actin, throughout early and mid-gestation stages of development in control ('C') or *Tbx5*-injected ('T') stage-matched embryos. All samples are derived from a single batch of eggs and identical results were achieved in at least two independent sets of experiments for each marker. EF1-alpha was used as a control for all RT-PCR reactions.

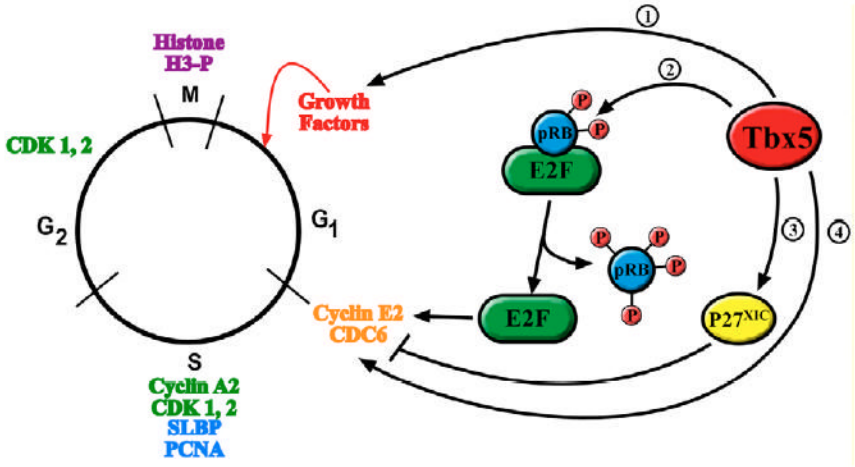

Fig. 7. Model for potential mechanisms by which TBX5 functions to control embryonic cardiac cell cycle progression

Schematic of embryonic cardiac cell cycle shown in left hand panel and potential roles for TBX5 in regulating G_1/S progression. (**1**) TBX5 may function to induce the expression of a growth factor, for example EGF or FGF required for cell cycle G_1 progression. (**2**) TBX5 may function to regulate E2F activity by controlling the phosphorylation state of pRB. (**3**) TBX5 could also negatively regulate general cell cycle inhibitors such as $p27^{Xic}$. (**4**) Alternatively TBX5 may function to regulate the expression of a key component of the CDK-cyclin complexes required for G_1/S progression.